



Published in final edited form as:

J Med Primatol. 2014 October ; 43(5): 298–309. doi:10.1111/jmp.12126.

Dysregulation of Multiple Inflammatory Molecules in Lymph Node and Ileum of Macaques during RT-SHIV Infection with or without Antiretroviral Therapy

Zandrea Ambrose^{1,*}, Christopher Kline¹, Patricia Polacino², and Shiu-Lok Hu^{2,3}

¹Division of Infectious Diseases, Department of Medicine, University of Pittsburgh School of Medicine, Pittsburgh, PA 15261

²Washington National Primate Research Center, University of Washington, Seattle, WA 98121

³Department of Pharmaceutics, University of Washington, Seattle, WA 98121

Abstract

Pathogenic infection with human immunodeficiency virus type 1 (HIV-1) or simian immunodeficiency virus (SIV) is characterized by a loss of CD4+ T cells and chronic lymphocyte activation even during suppressive antiretroviral therapy (ART). Using NanoString, expression of >100 molecules associated with inflammation or immune activation was evaluated in mesenteric lymph nodes and ileum of macaques infected with a pathogenic SIV/HIV virus, RT-SHIV, during viremia or during suppressive ART and compared to uninfected controls. Of the 105 RNA species quantified in the tissues, expression of 33 genes was altered significantly in one or both tissues during viremia but returned to normal levels during ART. However, 29 additional genes were altered in expression levels in the tissues of both viremic and ART-suppressed macaques.

Identification of the mechanisms of chronic inflammation in specific cells and in different tissues may help determine whether early ART initiation or novel therapies can prevent it.

Introduction

Infection with human immunodeficiency virus type 1 (HIV-1) is characterized by a loss of CD4+ T cells, the main targets for viral replication, as well as lymphocyte activation. Chronic inflammation is linked to disease progression and multiple organ damage during human immunodeficiency virus type 1 (HIV-1) infection¹. Immune activation and inflammation leads to abnormal collagen deposition in tissues, including in lymph nodes (LN) and in the gastrointestinal (GI) tract, of HIV-infected individuals^{2,3}. Although successful antiretroviral therapy (ART) can reduce plasma viremia to undetectable or extremely low levels, CD4+ T cell counts often do not return to normal in long-term ART-treated HIV+ individuals⁴. In addition, significant lymphocyte activation continues during viral suppression⁵ and normal architecture of tissues is not fully restored^{2,6}.

*Corresponding author: University of Pittsburgh School of Medicine 3550 Terrace Street 830 Scaife Hall Pittsburgh, PA 15261 zaa4@pitt.edu 412-624-0512 (telephone) 412-383-5851 (fax).

Chronic immune activation is correlated with persistent microbial translocation during HIV-1 infection, as measured by plasma lipopolysaccharide (LPS) levels⁷. Microbial translocation occurs after damage to the intestinal epithelium by many diseases, including HIV-1^{8,9}. Higher levels of many pro-inflammatory cytokines and type I interferon (IFN) in the blood and tissues have been associated with microbial translocation during HIV-1 infection compared to uninfected controls⁸. Both LPS and increased inflammatory molecules likely contribute to increased T cell activation seen in HIV+ individuals.

Control of chronic immune activation appears to correlate with decreased viral pathogenesis in nonhuman primate models of HIV-1. Similar to HIV infection in humans, pathogenic simian immunodeficiency virus (SIV) infection of rhesus macaques also showed severe depletion of intestinal CD4+ T cells during acute infection¹⁰ and microbial translocation associated with immune activation during chronic infection⁷. However, while SIV infection of natural hosts, such as sooty mangabeys and African green monkeys, results in severe acute mucosal CD4+ T cell depletion^{11,12}, there is no progression to pathogenesis or microbial translocation despite high viremia^{13,14}. Additionally, nonpathogenic SIV infection of natural hosts does not lead to an increase in activated lymphocytes in the blood or tissues. Furthermore, blocking specific pro-inflammatory molecules, such as TNF α ¹⁵, or altering immune regulation by administration of IL-7¹⁶ or anti-PD-1 antibodies¹⁷, during pathogenic SIV infection of rhesus macaques can decrease hyperimmune activation and microbial translocation.

In this study, a comprehensive analysis was performed of over 100 molecules associated with inflammation and immune activation in mesenteric LN and small intestine of pigtailed macaques infected with a pathogenic SIV/HIV chimeric virus, RT-SHIV_{mne27}¹⁸, while viremic or during suppressive ART and compared to uninfected controls. RNA expression of these factors was quantified in each sample by NanoString technology. As expected, significant immune dysregulation was observed during infection that did not return to normal after virus suppression.

Materials and Methods

Humane Care Guidelines

Experimental procedures on thirteen pigtailed macaques (*Macaca nemestrina*) used in the study were performed at the National Institutes of Health in a previous study¹⁹, and at the Washington National Primate Center, in both a previous¹⁸ and a new study, with approval by both Institutional Animal Care and Use Committees. The animals were negative for simian type D retrovirus and simian immunodeficiency virus and were cared for in accordance with established National Institutes of Health guidelines.

RT-SHIV infection and ART treatment of macaques

The derivation of the RT-SHIV_{mne027} stock was previously described¹⁸. Four animals were left uninfected and nine animals were infected intravenously with 1×10^5 infectious units as determined on TZM-bl cells. Five of the infected animals were treated with a brief nonsuppressive antiretroviral regimen during the study but remained viremic throughout the

study, including at the time of necropsy, which was performed 26 to 49 weeks post-infection. The other four infected animals received daily suppressive ART for 17-18 weeks and had undetectable plasma viremia at necropsy (30 to 46 weeks post-infection). The suppressive ART regimens contained 4 antiretroviral drugs consisting of tenofovir (20 mg/kg once per day subcutaneously) and L-870812 (100 mg twice per day orally) with either 1) darunavir/ritonavir (375 mg/50 mg twice per day orally) or 2) emtricitabine/efavirenz (40mg/kg and 400mg once per day subcutaneously and orally, respectively).

Blood and tissue RT-SHIV RNA isolation and quantitation

Peripheral blood, mesenteric lymph nodes (LN) and portions of small intestine (ileum in all cases except jejunum for one uninfected macaque) were removed from each animal at the time of necropsy. Plasma was separated by centrifugation and stored at -80°C until RNA extraction, while tissues were flash frozen in liquid nitrogen until RNA extraction. RNA was extracted as previously described from plasma^{20,21} and tissues¹⁹.

Viral RNA was quantified by quantitative RT-PCR (qPCR) using RT-SHIV *gag*-specific primers as previously described for plasma^{20,21} and tissues¹⁹.

NanoString

Expression analysis was performed by custom digital molecular barcoding using the NanoString nCounter® System (NanoString Technologies Inc., Seattle, WA)²². A custom CodeSet was designed against 120 inflammatory and immune marker genes and 5 “housekeeping” genes in rhesus macaque (*Macaca mulatta*). Each assay also contained 14 External RNA Controls Consortium (ERCC) transcript sequences as positive (n=6) and negative (n=8) hybridization controls. Total RNA samples were normalized to 100ng of input RNA in 5µl and were hybridized with reporter and capture probes at 65°C for 16h according to the manufacturer's directions. Samples were immediately transferred to the NanoString nCounter® Prep Station for automatic removal of excess probes and non-target RNA, immobilization of the sample on the assay cartridge, and electrophoresis to linearize hybrids for barcode counting. Cartridges were placed onto the NanoString nCounter® Digital Analyzer where images of the immobilized fluorescent reporters are collected by a CCD camera focused through a microscope objective lens. Images were collected for 600 fields of view per sample and processed for data export. Normalization and data analysis was carried out with the NanoString nCounter® Analysis Software v1.1.

Statistics

Statistics were performed using Prism (GraphPad Software, San Diego, CA). For comparisons of groups, unpaired t tests with 95% confidence intervals were used. For comparing viral RNA levels to host RNA levels, two-tailed Spearman nonparametric correlation with 95% confidence intervals was used.

Results

RT-SHIV RNA is significantly reduced in plasma and tissues during ART

To evaluate the expression of inflammatory genes in tissues of macaques during active RT-SHIV infection and during ongoing suppressive ART, blood and tissues were collected from uninfected controls and RT-SHIV-infected animals that remained viremic or that were treated with combination ART. Both LN and small intestine were chosen because they have been shown to harbor RT-SHIV-infected cells both during active replication of virus and during ART treatment^{19,23}. Plasma viral RNA levels showed that all RT-SHIV-infected macaques had high viremia at week 2 post-infection (Figure 1A). The infected, untreated animals remained viremic with high plasma RT-SHIV RNA levels at the time of necropsy (26-49 weeks post-infection), whereas the ART-treated animals had undetectable plasma viremia at necropsy after 17-18 weeks of treatment (30-46 weeks post-infection; Figure 1A).

We collected mesenteric LN from uninfected (n=5), viremic (n=6), and ART-suppressed (n=3) macaques. We collected ileum from uninfected (n=3), viremic (n=6), and ART-suppressed (n=4) macaques. The RNA isolated from LN of the infected, untreated animals contained high levels of RT-SHIV RNA (range of 4.8×10^5 - 1.8×10^7 copies/100ng total RNA; Figure 1B). However, there was a greater than 2 log lower level of mean viral RNA in the LN of ART-suppressed animals (range of <10 - 7.2×10^4 copies/100ng total RNA; Figure 1B). And whereas high levels of RT-SHIV RNA were measured in the ileum of viremic animals (range of 3.4×10^3 - 1.3×10^6 copies/100ng total RNA), all but one animal had undetectable viral RNA in the ileum (range of <10 - 47 copies/100ng total RNA; Figure 1B). Two LN and ileum tissues from different locations were collected from an animal from each group and found to have differences in RT-SHIV RNA, suggesting that tissue sampling recovered different numbers of infected target cells (data not shown).

CD8 RNA is positively correlated with viral RNA in lymph nodes and ileum and CD4 RNA is negatively correlated with viral RNA in ileum

NanoString was used to measure the change in expression of over 100 RNAs associated with inflammation and immunity. Probes were designed to RNA encoding 5 putative housekeeping proteins (clatherin heavy chain 1, GAPDH, beta-glucuronidase, hypoxanthine phosphoribosyltransferase, and tubulin) and 120 RNA inflammatory and immune molecules. In addition, internal controls (8 negative and 6 positive) were included in each assay run. All 5 housekeeping RNAs were detected in all tissue samples and 105 inflammatory RNAs were detected in one or both tissues, which could be categorized as chemokines and their receptors, cytokines and their receptors, kinases, oxidative stress molecules, surface immune and homing markers, toll-like receptors (TLRs), TNF/TNFR family proteins, transcription factors, and miscellaneous (Figure 2A). Internal controls were detected as expected (data not shown). In contrast to many inflammatory RNA molecules that were upregulated in viremic animals, housekeeping RNA remained stable (<1.5 -fold change) in samples from untreated RT-SHIV-infected animals compared to uninfected controls or ART-suppressed animals (Figure 2B).

CD4 and CD8 RNA copies were measured by NanoString in each tissue and plotted against RT-SHIV gag RNA copies measured by qRT-PCR in the same samples (Figure 3). CD4 RNA copies were negatively correlated with viral RNA copies in mesenteric LN ($p=0.0006$; Figure 3A), such that animals with undetectable viral RNA (uninfected and ART-treated animals) had the highest CD4 levels and animals with higher viremia had the lowest CD4 levels. In contrast, CD8 RNA copies were positively correlated with viral RNA copies in mesenteric LN ($p=0.0196$; Figure 3B), suggesting that animals with the highest viremia had more antigen stimulation of cytotoxic T cells. Ileum samples showed no significant negative correlation between RT-SHIV RNA and CD4 RNA ($p=0.1664$; Figure 3C), but a positive correlation between viral RNA and CD8 RNA levels ($p=0.0027$; Figure 3D). The lack of apparent CD4 T cell loss in small intestine could be due to slow restoration of gastrointestinal CD4⁺ T cells during ART^{24,25} or differential sampling of Peyer's patches.

Many inflammatory proteins are dysregulated in tissues after RT-SHIV infection but return to normal during ART

RT-SHIV infection of macaques led to significant changes in expression of many RNA molecules associated with inflammation in LN and ileum compared to uninfected controls. The expression levels returned to normal after suppression of viremia by ART (Tables 1 and 2). For example, CD103, also known as integrin αE and expressed on the majority of intraepithelial lymphocytes in the gut and dendritic cells in the gut and mesenteric LN²⁶, was significantly higher in LNs of untreated infected macaques than LNs of both uninfected and ART-treated RTSHIV+ macaques (Figure 4A). Similar to CD8, CD103 expression correlated positively with RTSHIV gag copies in LN ($p=0.0042$; Figure 4B). In LN, 13 genes were downregulated and 12 genes were upregulated in RT-SHIV+ animals that returned to normal during ART suppression (Table 1). In ileum, 5 genes were downregulated and 12 genes were upregulated after infection that returned to normal during ART (Table 2). Two molecules (MAPK8 and TRAF2) were downregulated and 7 molecules (CCL3, CCL4, CCL5, CXCL9, CXCL10, CD8 and STAT1) were upregulated in both tissues.

Many inflammatory proteins are dysregulated in tissues after RT-SHIV infection in the presence and absence of ART suppression

Some inflammatory molecules were dysregulated after RT-SHIV infection and did not return to normal levels after 17-18 weeks of suppressive ART (Tables 3 and 4). For example, CD103 was significantly upregulated in ileum of both untreated and ART-treated RT-SHIV+ macaques (Figure 4C). While a positive correlation was observed between CD103 and gag RNA levels in ileum ($p=0.0477$; Figure 4D), the correlation was increased when data points from ART-treated animals with undetectable gag RNA levels were removed ($p=0.0083$; Figure 4E). Twenty-four molecules in the NanoString CodeSet were downregulated in the LN of infected animals, both treated and untreated (Table 3). Seven molecules were downregulated and 4 molecules were upregulated in the ileum after RT-SHIV infection (Table 4). Six downregulated genes were shared in both ileum and LN: CD40, CD40L, DAXX, GRB2, HLA-DRB1, and MAP3K5.

Some genes are altered in tissues during ART suppression

Interestingly, some inflammatory molecules were normal in LN and ileum after RTSHIV infection but changed after 17-18 weeks of ART (Tables 5 and 6). For example, protein kinase C beta (PRKCB) expression was not different in uninfected and untreated RT-SHIV+ macaques but was significantly decreased in ART-treated infected animals in both LN and ileum (Figure 5). Six genes in LN and 9 genes in ileum were downregulated in ART-suppressed macaques, including ATF2 and PRKCB in both tissues (Tables 5 and 6, respectively). In addition, members of the MEF2 family proteins were downregulated in both tissues of treated animals. One protein, MAP2K6, was upregulated in the ileum of ART-treated macaques (Table 6).

Discussion

Chronic immune activation during HIV-1 or SIV infection contributes to viral pathogenesis and tissue pathology even during suppression by ART. Many studies have focused on one or a subset of proteins involved in inflammation or immune regulation. We wanted to determine the expression levels of a large number of molecules that could contribute to hyperimmune activation both during active infection and during ART suppression. These included chemokines and their receptors, cytokines, kinases, oxidative stress molecules, surface immune and homing markers, TLRs, TNF/TNFR family proteins, and transcription factors. Of the 105 RNA species detected and quantified in LN and ileum by our NanoString CodeSet, several genes were down- or upregulated during viremia but returned to normal levels during ART. Not surprisingly, expression of many additional genes was altered in tissues of RT-SHIV-infected animals in both the presence and absence of ART suppression. However, while some RNAs were consistently up- or downregulated in both LN and ileum, many were unique to one tissue type, suggesting that dysregulation of innate immunity differed in the small intestine compared to lymphoid tissue.

As expected, many of the molecules that changed during infection included chemokines and cytokines and their receptors, integrins, CD4, CD8, CD68, and HLA-DR, which have been associated with chronic inflammation¹. In addition, some TLRs were upregulated after infection, which have been associated with innate immune responses to both viruses²⁷ and microbial translocation⁸. Not surprisingly, several kinases in the signaling pathway were altered, which could influence the expression of several pro-inflammatory molecules. Interestingly, transcription factors were altered during RT-SHIV infection, including during ART treatment. As transcription factors control latency and reactivation of proviral DNA²⁸, exploration of the expression levels of specific factors in tissues may give insight into the development and maintenance of lentiviral reservoirs.

Fifteen RNAs were not detected by the assay in both tissue types, which could be due to several factors. First, the probes designed to bind to these molecules may not be optimized. Or, it is possible that these RNAs are not present at detectable levels in total LN or ileum tissue RNA. Isolation of specific cell subsets may determine whether relatively few cells produce certain factors within a tissue type and would likely result in more significant changes in expression after infection. Indeed, *in situ* hybridization or protein staining may show inflammatory or innate immune responses in specific regions of a tissue²⁹ or in cells in

which active replication is occurring. Future studies should identify specific subsets of cells expressing increased or decreased levels of these molecules. In addition, infection of RT-SHIV in specific cell subsets or in the localized regions should be measured and correlated to change in RNA or protein expression levels of pro-inflammatory molecules.

A few genes were altered in LN (6) and ileum (10) only during ART treatment, which may be due to therapy. All of the treated animals received tenofovir and the integrase inhibitor L-870812, while the other drugs differed. Future studies may be necessary to compare larger groups of animals that receive specific treatment regimens to determine whether antiretroviral drugs influence inflammation in tissues. Similarly, levels of specific drugs in tissues or specific cell types may be required to understand this phenomenon. Finally, duration of ART may influence whether altered expression of some molecules returns to pre-infection levels.

In conclusion, we have demonstrated that NanoString can be successfully used to measure the levels of expression of multiple innate immune markers in the same tissue samples of macaques. Comparison of uninfected animals with RT-SHIV-infected animals showed significant changes in multiple RNAs associated with inflammation, which sometimes returned to normal after suppression of virus with ART. However, many RNAs did not return to normal levels during ART, suggesting that these pathways may be irreversibly damaged prior to treatment. Future studies identifying the mechanisms of inflammatory dysregulation in specific cell types in both the gut and lymphoid tissues will give insight into how hyperimmune activation occurs and perhaps whether early ART initiation or novel therapies can prevent chronic inflammation and microbial translocation.

Acknowledgments

The authors would like to thank Leon Flanary and Jeremy Smedley for veterinary support, the University of Pittsburgh Genomics and Proteomics Core Laboratories for performing NanoString assays, and Kathleen Shutt for statistical consultation. This study was supported by NIH R01 grant AI080290.

References

1. Lederman MM, Funderburg NT, Sekaly RP, Klatt NR, Hunt PW. Residual immune dysregulation syndrome in treated HIV infection. *Adv Immunol.* 2013; 119:51–83. [PubMed: 23886064]
2. Schacker TW, Nguyen PL, Beilman GJ, et al. Collagen deposition in HIV-1 infected lymphatic tissues and T cell homeostasis. *J Clin Invest.* Oct; 2002 110(8):1133–1139. [PubMed: 12393849]
3. Estes J, Baker JV, Brenchley JM, et al. Collagen deposition limits immune reconstitution in the gut. *J Infect Dis.* Aug 15; 2008 198(4):456–464. [PubMed: 18598193]
4. Kelley CF, Kitchen CM, Hunt PW, et al. Incomplete peripheral CD4+ cell count restoration in HIV-infected patients receiving long-term antiretroviral treatment. *Clin Infect Dis.* Mar 15; 2009 48(6): 787–794. [PubMed: 19193107]
5. Hunt PW, Martin JN, Sinclair E, et al. T cell activation is associated with lower CD4+ T cell gains in human immunodeficiency virus-infected patients with sustained viral suppression during antiretroviral therapy. *J Infect Dis.* May 15; 2003 187(10):1534–1543. [PubMed: 12721933]
6. Schacker TW, Nguyen PL, Martinez E, et al. Persistent abnormalities in lymphoid tissues of human immunodeficiency virus-infected patients successfully treated with highly active antiretroviral therapy. *J Infect Dis.* Oct 15; 2002 186(8):1092–1097. [PubMed: 12355359]

7. Brenchley JM, Price DA, Schacker TW, et al. Microbial translocation is a cause of systemic immune activation in chronic HIV infection. *Nat Med*. Dec; 2006 12(12):1365–1371. [PubMed: 17115046]
8. Sandler NG, Douek DC. Microbial translocation in HIV infection: causes, consequences and treatment opportunities. *Nat Rev Microbiol*. Sep; 2012 10(9):655–666. [PubMed: 22886237]
9. Marchetti G, Tincati C, Silvestri G. Microbial translocation in the pathogenesis of HIV infection and AIDS. *Clin Microbiol Rev*. Jan; 2013 26(1):2–18. [PubMed: 23297256]
10. Veazey RS, DeMaria M, Chalifoux LV, et al. Gastrointestinal tract as a major site of CD4+ T cell depletion and viral replication in SIV infection. *Science*. Apr 17; 1998 280(5362):427–431. [PubMed: 9545219]
11. Gordon SN, Klatt NR, Bosinger SE, et al. Severe depletion of mucosal CD4+ T cells in AIDS-free simian immunodeficiency virus-infected sooty mangabeys. *J Immunol*. Sep 1; 2007 179(5):3026–3034. [PubMed: 17709517]
12. Pandrea IV, Gautam R, Ribeiro RM, et al. Acute loss of intestinal CD4+ T cells is not predictive of simian immunodeficiency virus virulence. *J Immunol*. Sep 1; 2007 179(5):3035–3046. [PubMed: 17709518]
13. Paiardini M, Frank I, Pandrea I, Apetrei C, Silvestri G. Mucosal immune dysfunction in AIDS pathogenesis. *AIDS Rev*. Jan-Mar; 2008 10(1):36–46. [PubMed: 18385779]
14. Estes JD, Harris LD, Klatt NR, et al. Damaged intestinal epithelial integrity linked to microbial translocation in pathogenic simian immunodeficiency virus infections. *PLoS Pathog*. 2010; 6(8):e1001052. [PubMed: 20808901]
15. Tabb B, Morcock DR, Trubey CM, et al. Reduced inflammation and lymphoid tissue immunopathology in rhesus macaques receiving anti-tumor necrosis factor treatment during primary simian immunodeficiency virus infection. *J Infect Dis*. Mar 15; 2013 207(6):880–892. [PubMed: 23087435]
16. Sereti I, Estes JD, Thompson WL, et al. Decreases in Colonic and Systemic Inflammation in Chronic HIV Infection after IL-7 Administration. *PLoS Pathog*. Jan. 2014 10(1):e1003890. [PubMed: 24497828]
17. Dyavar Shetty R, Velu V, Titanji K, et al. PD-1 blockade during chronic SIV infection reduces hyperimmune activation and microbial translocation in rhesus macaques. *J Clin Invest*. May 1; 2012 122(5):1712–1716. [PubMed: 22523065]
18. Ambrose Z, Palmer S, Boltz VF, et al. Suppression of viremia and evolution of human immunodeficiency virus type 1 drug resistance in a macaque model for antiretroviral therapy. *J Virol*. Nov; 2007 81(22):12145–12155. [PubMed: 17855539]
19. Kline C, Ndjomou J, Franks T, et al. Persistence of Viral Reservoirs in Multiple Tissues after Antiretroviral Therapy Suppression in a Macaque RT-SHIV Model. *PLoS One*. 2013; 8(12):e84275. [PubMed: 24367650]
20. Cline AN, Bess JW, Piatak M Jr, Lifson JD. Highly sensitive SIV plasma viral load assay: practical considerations, realistic performance expectations, and application to reverse engineering of vaccines for AIDS. *J Med Primatol*. Oct; 2005 34(5-6):303–312. [PubMed: 16128925]
21. Polacino P, Cleveland B, Zhu Y, et al. Immunogenicity and protective efficacy of Gag/Pol/Env vaccines derived from temporal isolates of SIVmne against cognate virus challenge. *J Med Primatol*. Aug; 2007 36(4-5):254–265. [PubMed: 17669214]
22. Geiss GK, Bumgarner RE, Birditt B, et al. Direct multiplexed measurement of gene expression with color-coded probe pairs. *Nat Biotechnol*. Mar; 2008 26(3):317–325. [PubMed: 18278033]
23. North TW, Higgins J, Deere JD, et al. Viral sanctuaries during highly active antiretroviral therapy in a nonhuman primate model for AIDS. *J Virol*. Mar; 2010 84(6):2913–2922. [PubMed: 20032180]
24. Guadalupe M, Reay E, Sankaran S, et al. Severe CD4+ T-cell depletion in gut lymphoid tissue during primary human immunodeficiency virus type 1 infection and substantial delay in restoration following highly active antiretroviral therapy. *J Virol*. Nov; 2003 77(21):11708–11717. [PubMed: 14557656]

25. Mehandru S, Poles MA, Tenner-Racz K, et al. Mechanisms of gastrointestinal CD4+ T-cell depletion during acute and early human immunodeficiency virus type 1 infection. *J Virol.* Jan; 2007 81(2):599–612. [PubMed: 17065209]
26. Gorfu G, Rivera-Nieves J, Ley K. Role of beta7 integrins in intestinal lymphocyte homing and retention. *Curr Mol Med.* Sep; 2009 9(7):836–850. [PubMed: 19860663]
27. Thompson AJ, Locarnini SA. Toll-like receptors, RIG-I-like RNA helicases and the antiviral innate immune response. *Immunol Cell Biol.* Aug-Sep;2007 85(6):435–445. [PubMed: 17667934]
28. Taube R, Peterlin M. Lost in transcription: molecular mechanisms that control HIV latency. *Viruses.* Mar; 2013 5(3):902–927. [PubMed: 23518577]
29. Choi YK, Fallert BA, Murphey-Corb MA, Reinhart TA. Simian immunodeficiency virus dramatically alters expression of homeostatic chemokines and dendritic cell markers during infection in vivo. *Blood.* Mar 1; 2003 101(5):1684–1691. [PubMed: 12406887]

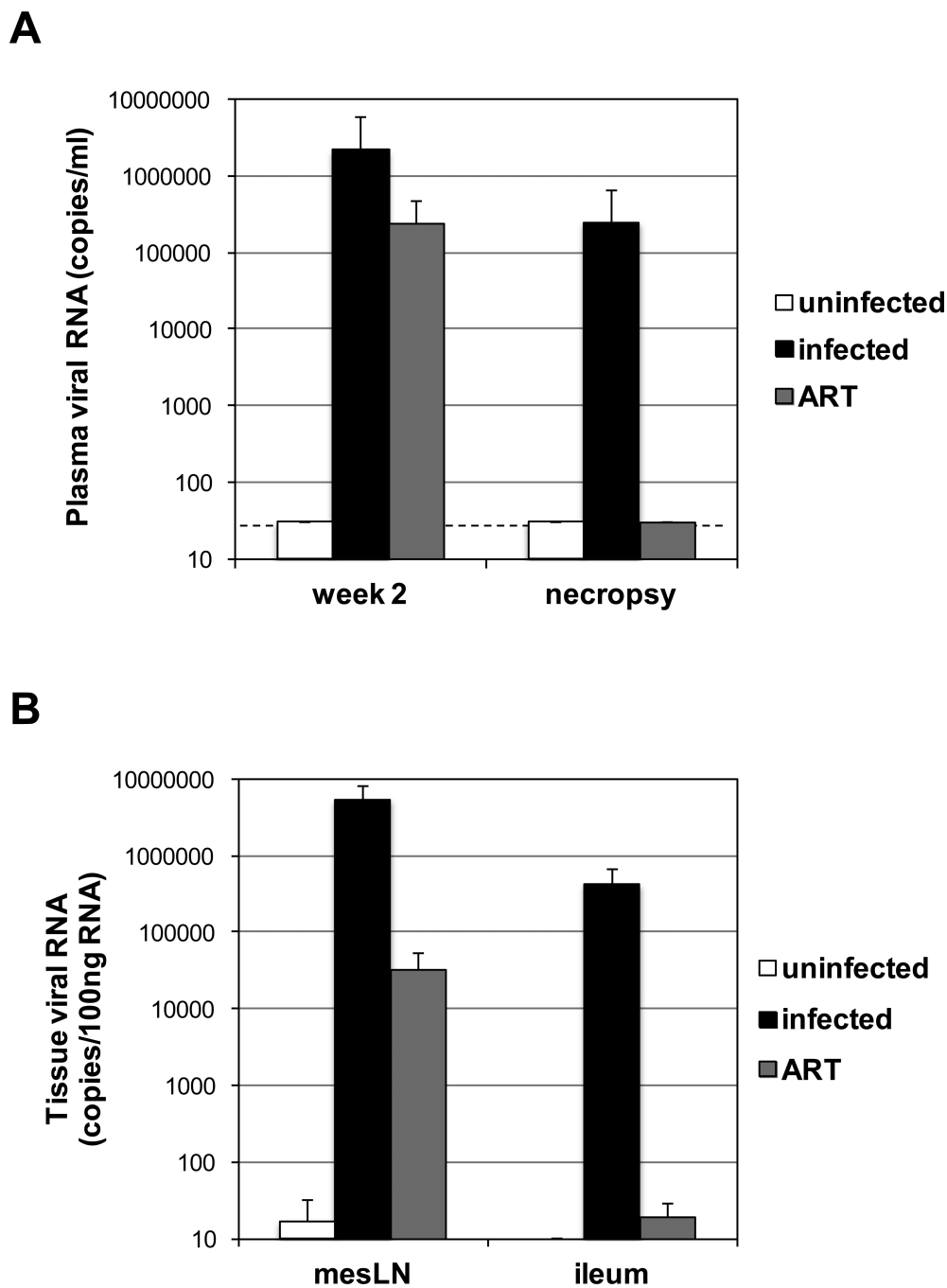


Figure 1. (A) Plasma viral RNA detected at week 2 post-infection and necropsy from the uninfected animals, untreated RT-SHIV-infected animals, and ART-treated RT-SHIV-infected animals. The dotted line denotes the limit of detection of 30 viral RNA copies/ml. (B) Viral RNA detected in mesenteric LN and ileum samples of uninfected animals, untreated RT-SHIV-infected animals, and ART-treated RT-SHIV-infected animals is graphed per 100ng of total tissue RNA. Each bar represents the median of all samples in each group and error bars represent standard deviations.

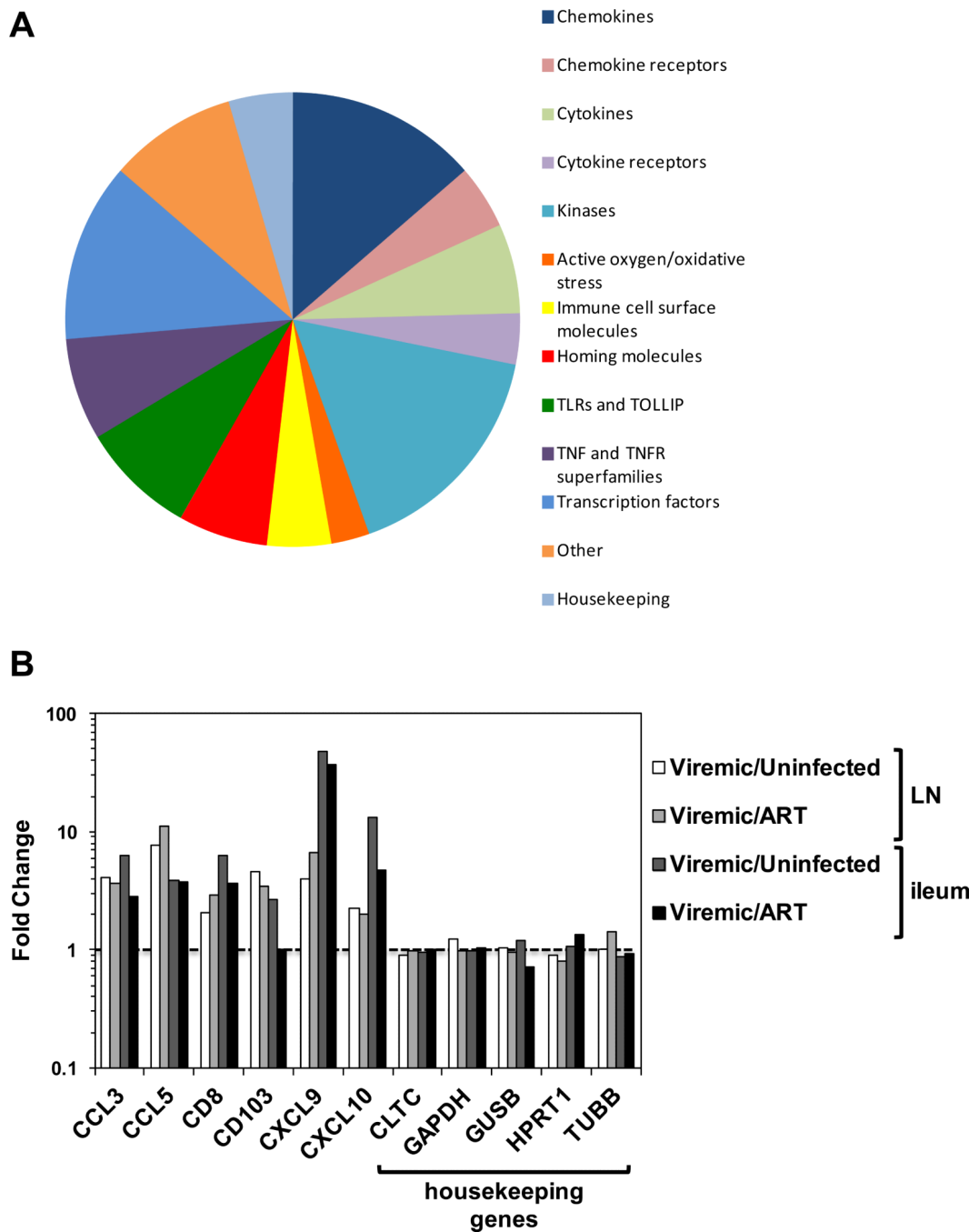


Figure 2. (A) The proportion of the NanoString CodeSet in each category of gene products detected in the samples (total = 110). (B) Results are shown of a subset of inflammatory RNA molecules and all 5 housekeeping RNA molecules measured in mesenteric LN and ileum from all samples. The results were averaged per group and the fold difference between viremic (untreated infected) animals or ART-treated animals and uninfected controls. The dotted line denotes no difference or a fold change of 1.

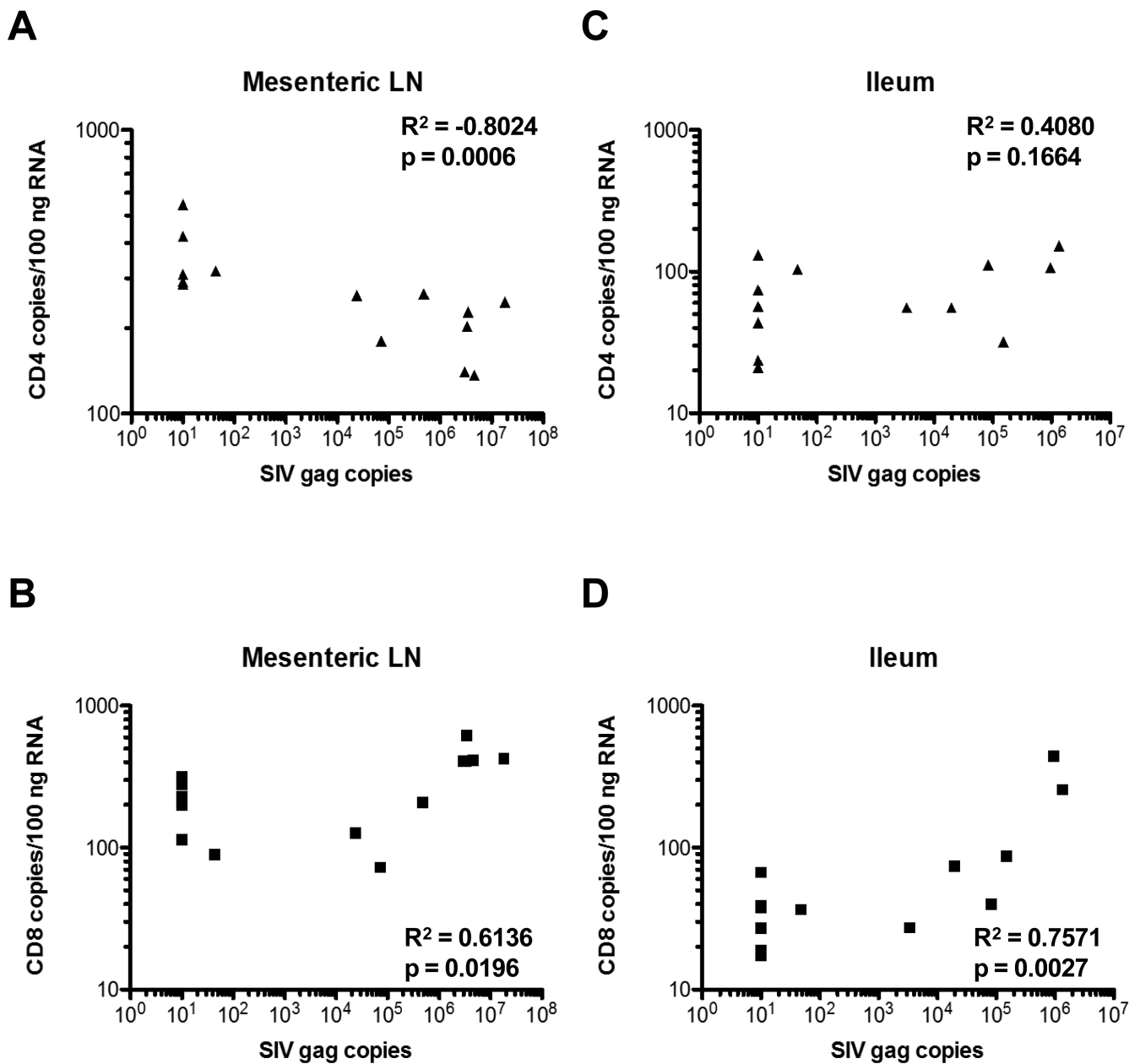


Figure 3. CD4 RNA copies/100ng RNA in (A) mesenteric LN and (C) ileum and CD8 RNA copies/100ng RNA in (B) mesenteric LN and (D) ileum were plotted against SIV gag copies detected in the same samples. R^2 and p values were determined by Spearman correlation.

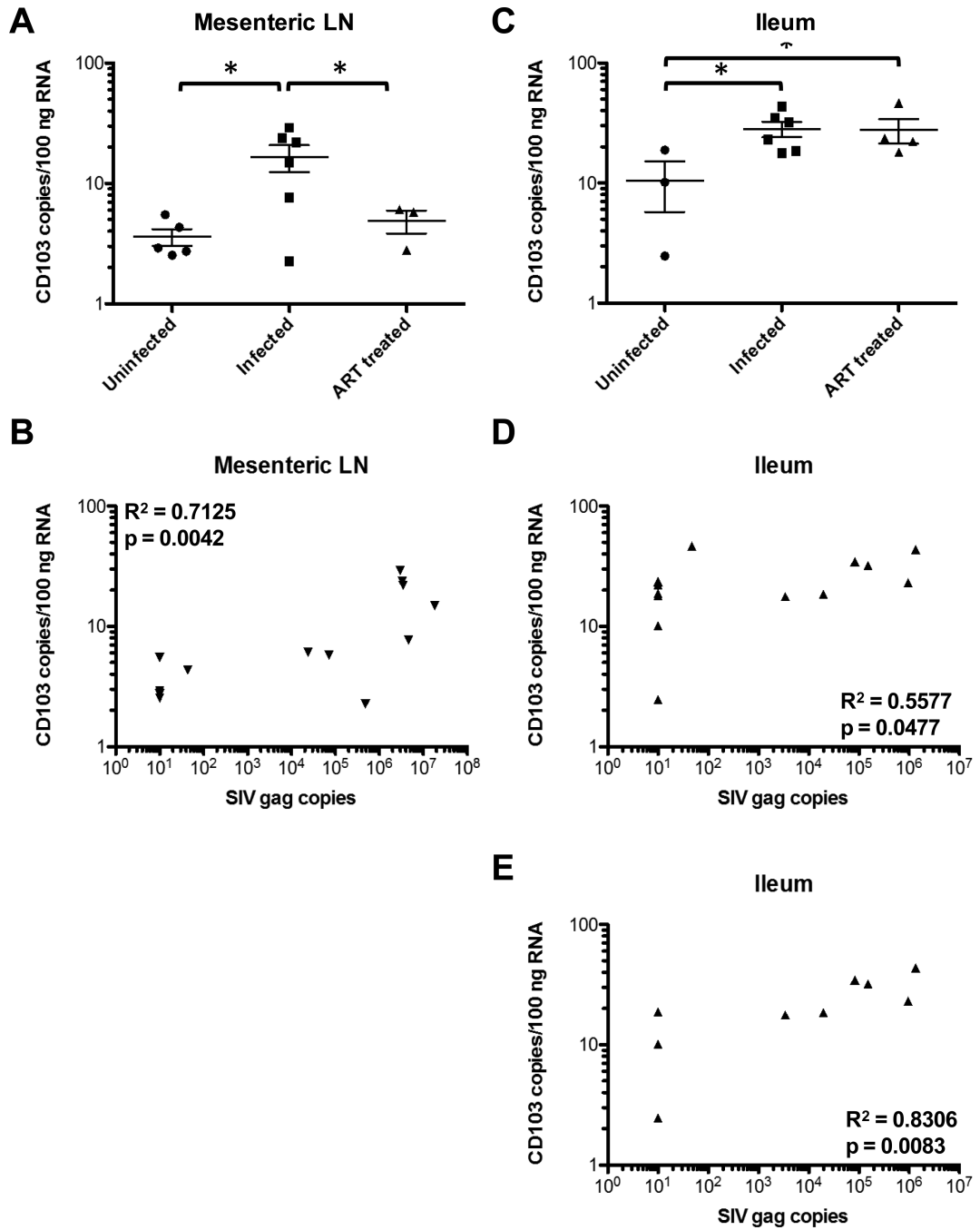


Figure 4. CD103, or integrin αE , RNA copies in (A) mesenteric LN and (C) ileum of uninfected, untreated RT-SHIV+, and ART-treated RT-SHIV+ macaques. Asterisks denote p values < 0.05 between groups determined by unpaired t tests. CD103 RNA copies/100ng RNA in (B) mesenteric LN and (D) ileum were plotted against SIV gag copies detected in all animals. (E) CD103 RNA copies/100ng RNA in ileum of only uninfected and untreated RT-SHIV+ macaques. R^2 and p values were determined by Spearman correlation.

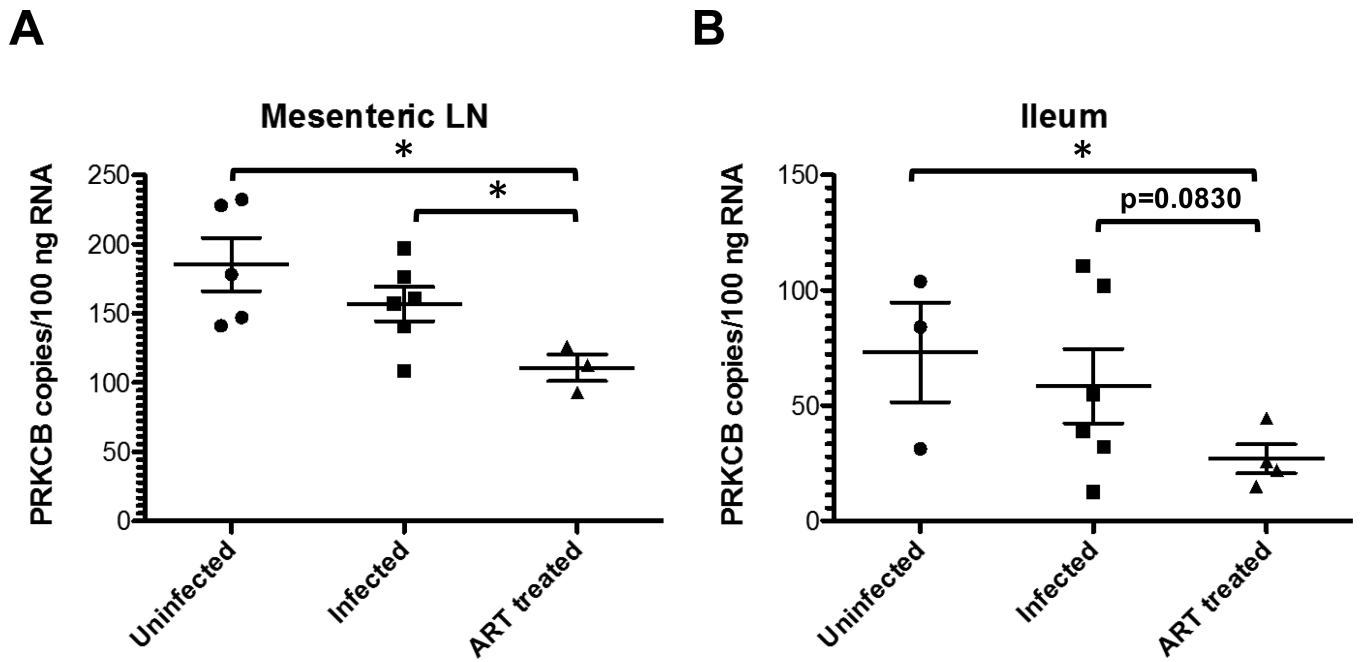


Figure 5. PRKCB RNA copies in (A) mesenteric LN and (C) ileum of uninfected, untreated RTSHIV+, and ART-treated RT-SHIV+ macaques. Asterisks denote p values < 0.05 between groups determined by unpaired t tests.

Table 1

RNA copies altered in LN of RT-SHIV-infected macaques, but normal in ART-suppressed RT-SHIV-infected macaques.

Gene	Copy Number Average (SEM)			t Test p Values			Spearman Correlation p Values
	Uninfected	Infected	ART	Uninfected v. Infected	Infected v. ART	Uninfected v. ART	
CCL17	230 (42)	86 (22)	155 (49)	0.0054	0.0866	0.1796	0.1170
CCL21	5479 (1230)	2033 (502)	6178 (4112)	0.0108	0.0905	0.4224	0.0050
CCR4	104 (23)	40 (6)	57 (3)	0.0085	0.0604	0.0879	0.0596
CD4	326 (25)	203 (22)	329 (111)	0.0025	0.0789	0.4842	0.0006
IL-1R	55 (13)	37 (3)	52 (2)	0.0951	0.0075	0.4334	0.1010
LTB	328 (37)	208 (55)	462 (315)	0.0601	0.1442	0.2938	0.0233
MAP2K6	54 (9)	34 (5)	44 (15)	0.0335	0.2017	0.2861	0.0154
<u>MAPK8</u>	64 (7)	44 (2)	52 (4)	0.0064	0.0347	0.1196	0.0104
MAPKAPK5	57 (6)	45 (4)	54 (17)	0.0688	0.2385	0.4309	0.0833
MYC	199 (14)	180 (16)	262 (60)	0.2020	0.0577	0.1144	0.0476
NFATc3	214 (22)	147 (12)	211 (54)	0.0105	0.0743	0.4751	0.0321
TLR5	11 (3)	6 (0.8)	9 (2)	0.0391	0.0292	0.3225	0.0650
<u>TRAF2</u>	49 (4)	38 (7)	43 (16)	0.1064	0.3687	0.3272	0.0454
<u>CCL3</u>	26 (6)	99 (18)	27 (3)	0.0032	0.0148	0.4511	0.0011
<u>CCL4</u>	67 (11)	192 (32)	55 (16)	0.0039	0.0120	0.2707	0.0208
<u>CCL5</u>	24 (5)	186 (25)	17 (1)	0.0001	0.0011	0.1399	0.0025
<u>CXCL9</u>	360 (232)	1433 (332)	215 (95)	0.0160	0.0210	0.3317	0.0023
<u>CXCL10</u>	335 (224)	743 (163)	373 (22)	0.0828	0.0826	0.4509	0.0305
CCR5	19 (3)	35 (6)	13 (2)	0.0324	0.0258	0.1324	0.0623
<u>CD8</u>	199 (44)	413 (53)	143 (46)	0.0073	0.0071	0.2185	0.0196
FasL	16 (3)	29 (6)	12 (3)	0.0395	0.0416	0.1726	0.0356
integrin α E	4 (1)	17 (4)	5 (1)	0.0104	0.0493	0.1408	0.0042
IL-15	68 (12)	35 (3)	55 (9)	0.0104	0.0187	0.2405	0.0050
JUN	27 (7)	43 (8)	26 (6)	0.0794	0.1058	0.4753	0.0246
<u>STAT1</u>	498 (154)	684 (90)	456 (13)	0.1524	0.0646	0.4225	0.0936

Bold, p value < 0.05

Underline, RNA altered similarly in ileum

Table 2

RNA copies altered in ileum of RT-SHIV-infected macaques, but normal in ART-suppressed RT-SHIV-infected macaques.

Gene	Copy Number Average (SEM)			t Test p Values			Spearman Correlation p Values
	Uninfected	Infected	ART	Uninfected v. Infected	Infected v. ART	Uninfected v. ART	
<u>MAPK8</u>	60 (6)	50 (6)	83 (10)	0.1513	0.0084	0.0789	0.0143
MEF2D	53 (1)	33 (4)	74 (45)	0.0094	0.1453	0.3506	0.0550
PLCB1	52 (10)	30 (5)	46 (24)	0.0323	0.2304	0.4214	0.2174
Raf-1	111 (8)	95 (9)	132 (22)	0.1531	0.0558	0.2339	0.0107
<u>TRAF2</u>	54 (11)	43 (5)	78 (20)	0.1523	0.0351	0.1951	0.0759
CCL2	12 (4)	47 (8)	32 (14)	0.0114	0.1599	0.1440	0.0181
<u>CCL3</u>	6 (2)	39 (16)	14 (8)	0.0950	0.1248	0.2261	0.0329
<u>CCL4</u>	64 (17)	114 (31)	44 (13)	0.1621	0.0600	0.1925	0.0566
<u>CCL5</u>	25 (7)	97 (36)	26 (4)	0.1053	0.0747	0.4541	0.0374
<u>CXCL9</u>	16 (3)	756 (443)	21 (10)	0.1459	0.1106	0.3519	0.0004
<u>CXCL10</u>	21 (6)	280 (88)	59 (22)	0.0425	0.0414	0.1108	0.0008
<u>CD8</u>	25 (7)	154 (66)	43 (9)	0.1123	0.1082	0.0923	0.0027
integrin β 7	14 (7)	27 (7)	9 (3)	0.1497	0.0367	0.2215	0.0203
MAP2K4	69 (6)	99 (10)	56 (15)	0.0497	0.0206	0.2533	0.0117
<u>STAT1</u>	171 (19)	392 (62)	203 (46)	0.0235	0.0292	0.3014	0.0068
TLR7	19 (12)	26 (4)	16 (6)	0.2307	0.0720	0.4131	0.0234
TLR8	17 (4)	24 (8)	11 (5)	0.2741	0.1271	0.2395	0.0381

Bold, p value < 0.05

Underline, RNA altered similarly in LN

Table 3

RNA copies downregulated in LN of both RT-SHIV-infected and ART-suppressed RT-SHIV-infected macaques.

Gene	Copy Number Average (SEM)			t Test p Values			Spearman Correlation p Values*
	Uninfected	Infected	ART	Uninfected v. Infected	Infected v. ART	Uninfected v. ART	
CCL22	29 (5)	10 (3)	15 (3)	0.0017	0.1120	0.0374	0.0306
CCR2	22 (5)	11 (2)	8 (4)	0.0225	0.2733	0.0438	0.0277
CCR7	582 (61)	269 (51)	315 (84)	0.0016	0.3166	0.0199	0.1142
CD40	153 (12)	99(13)	69 (9)	0.0066	0.0796	0.0014	0.1375
<u>CD40L</u>	138 (10)	61 (13)	90 (20)	0.0006	0.1214	0.0236	0.0144
CREB-1	293 (23)	214 (13)	176 (24)	0.0061	0.0868	0.0082	0.0226
<u>DAXX</u>	50 (4)	39 (6)	32 (6)	0.0710	0.2458	0.0168	0.1359
<u>GRB2</u>	244 (23)	184 (11)	134 (7)	0.0162	0.0102	0.0058	0.1316
HLA-DRA	5049 (357)	3893 (339)	2876 (522)	0.0220	0.0678	0.0059	0.1635
<u>HLA-DRB1</u>	958 (452)	28 (18)	32 (15)	0.0243	0.4463	0.0875	0.0112
IL-6R	194 (19)	110 (12)	115 (12)	0.0017	0.3834	0.0125	0.0204
IL-23A	21 (2)	10 (2)	11 (5)	0.0009	0.3516	0.0489	0.0393
LTA	13 (2)	9 (1)	5 (2)	0.0614	0.0613	0.0218	0.1142
MAP3K1	213 (30)	142 (18)	127 (16)	0.0314	0.3103	0.0422	0.3560
<u>MAP3K5</u>	152 (21)	108 (11)	116 (11)	0.0423	0.3388	0.1310	0.1546
MAP3K7	109 (7)	81 (7)	68 (12)	0.0130	0.1721	0.0095	0.2483
MEF2A	120 (15)	85 (6)	77 (2)	0.0232	0.2006	0.0375	0.1294
MEF2C	74 (9)	54 (8)	31 (7)	0.0587	0.0593	0.0076	0.4348
NFE2L2	114 (17)	86 (10)	82 (4)	0.0762	0.3934	0.0978	0.3560
NFKB1	113 (15)	80 (10)	72 (12)	0.0432	0.3227	0.0507	0.3863
NR3C1	179 (15)	131 (19)	99 (25)	0.0443	0.1816	0.0126	0.3863
PTK2	70 (7)	50 (7)	29 (10)	0.0351	0.0634	0.0068	0.2608
TLR6	86 (17)	56 (4)	54 (11)	0.0440	0.4102	0.1095	0.1072
TRADD	90 (11)	58 (4)	49 (9)	0.0075	0.1670	0.0192	0.0939

Bold, p value < 0.05

Underline, RNA also downregulated significantly in ileum

Table 4

RNA copies altered in ileum of both RT-SHIV-infected macaques and ART-suppressed RT-SHIV-infected macaques.

Gene	Copy Number Average (SEM)			t Test p Values			Spearman Correlation p Values*
	Uninfected	Infected	ART	Uninfected v. Infected	Infected v. ART	Uninfected v. ART	
<u>CD40</u>	65 (21)	37 (13)	13 (3)	0.1385	0.0856	0.0170	0.2696
<u>CD40L</u>	22 (3)	6 (2)	8 (4)	0.0010	0.3735	0.0204	0.0255
<u>DAXX</u>	47 (10)	20 (4)	21 (2)	0.0072	0.4357	0.0136	0.0138
<u>GRB2</u>	180 (16)	138 (15)	87 (25)	0.0603	0.0477	0.0174	0.0666
<u>HLA-DRB1</u>	361 (257)	60 (52)	101 (43)	0.0734	0.2932	0.1466	0.3586
<u>MAP3K5</u>	87 (20)	61 (5)	47 (8)	0.0688	0.0780	0.0450	0.3586
TGFB2	44 (16)	21 (9)	13 (4)	0.1010	0.2550	0.0396	0.2298
CCL2	12 (4)	47 (8)	32 (14)	0.0114	0.1599	0.1440	0.0083
CD68	43 (10)	77 (9)	86 (21)	0.0304	0.3320	0.0818	0.0760
integrin α E	11 (5)	28 (4)	28 (6)	0.0174	0.4679	0.0500	0.0083
TLR3	13 (3)	35 (5)	29 (7)	0.0141	0.2380	0.0674	0.4101

Bold, p value < 0.05

Underline, RNA also downregulated significantly in LN

Table 5

RNA copies downregulated in LN of ART-suppressed RT-SHIV-infected macaques, but normal in untreated RT-SHIV-infected macaques.

Gene	Copy Number Average (SEM)			t Test p Values			Spearman Correlation p Values*
	Uninfected	Infected	ART	Uninfected v. Infected	Infected v. ART	Uninfected v. ART	
<u>ATF2</u>	136 (19)	123 (13)	78 (26)	0.2928	0.0610	0.0579	0.0968
E-cadherin	73 (13)	57 (11)	33 (6)	0.1794	0.0860	0.0318	0.0061
MEF2D	75 (12)	61 (7)	40 (8)	0.1672	0.0451	0.0410	0.0255
TNF α	39 (8)	48 (12)	20 (3)	0.2830	0.0801	0.0544	0.0968
<u>PRKCB</u>	185 (19)	157 (12)	111 (10)	0.1150	0.0238	0.0157	0.0083
TOLLIP	74 (7)	67 (8)	45 (3)	0.2536	0.0521	0.0125	0.0589

Bold, p value < 0.05

Underline, RNA also downregulated significantly in ileum

Table 6

RNA copies altered in ileum of ART-suppressed RT-SHIV-infected macaques, but normal in untreated RT-SHIV-infected macaques.

Gene	Copy Number Average (SEM)			t Test p Values			Spearman Correlation p Values*
	Uninfected	Infected	ART	Uninfected v. Infected	Infected v. ART	Uninfected v. ART	
<u>ATF2</u>	95 (6)	88 (10)	64 (13)	0.3344	0.0796	0.0513	0.3679
CCR1	25 (7)	26 (6)	10 (2)	0.4438	0.0308	0.0322	0.0126
CD44	286 (79)	283 (60)	109 (12)	0.4891	0.0246	0.0229	0.0088
MAPK8	60 (6)	50 (6)	83 (10)	0.1513	0.0084	0.0789	0.0072
MEF2A	150 (7)	109 (20)	88 (2)	0.1011	0.2070	<0.0001	0.8113
MEF2C	34 (14)	22 (6)	9 (1)	0.1772	0.0455	0.0379	0.1231
NR3C1	97 (18)	85 (9)	60 (6)	0.2633	0.0407	0.0385	0.2788
<u>PRKCB</u>	73 (22)	59 (16)	27 (6)	0.3066	0.0830	0.0325	0.0963
TLR2	16 (8)	23 (7)	7 (3)	0.2483	0.0435	0.1360	0.0202
MAP2K6	41 (4)	40 (7)	102 (16)	0.4567	0.0017	0.0119	0.0202

Bold, p value < 0.05

Underline, RNA also downregulated significantly in LN